DEFORMATION ANALYSES OF GABION STRUCTURES

Der-Guey Lin[1]*, Bor-Shun Huang[2], Shin-Hwei Lin[3]

ABSTRACT

This study proposed a numerical procedure to simulate the deformation behaviors of the uniaxial compression test of single gabion and of the lateral loading test of full scale gabion retaining wall. The validity of the numerical procedures is verified by the comparison of the measurements with the simulations of deformation behavior. In addition, two evaluation equations which are capable of estimating the horizontal and the vertical displacement of the front face of laterally loaded gabion structure are presented for engineering practice. The numerical results indicates the deformation mode of a loaded gabion structure can be effectively captured in numerical model when incorporating a structural beam element with limit axial stiffness and relatively low or zero flexural stiffness. It is also found that the apparent total shear modulus of gabion structure, which has taken the compound shear deformation behavior of wire mesh and infilled stone into account, should be adopted in numerical modeling instead of using the shear modulus of infilled stone itself.

Key Words：Gabion structures, Apparent total shear modulus, Evaluation equations

INTRODUCTION

In Taiwan, various ecological engineering working methods were introduced into many reconstruction projects in the disastrous area of the 921 Quake occurred in 1999. Due to the features of high flexibility, high permeability and high roughness gabion structures were considered as an alternative construction method to meet the demand of ecological criteria. As a result, in the recent year gabion structures were commonly used for the constructions of revetment and retaining wall.

For a loaded gabion structure, a compound type of deformation comprised of the horizontal shear displacement and the vertical compression displacement can be observed. However, it was difficult to evaluate the deformations resulted from the interactions of earth pressure/gabion structure/foundation soil simply using the conventional mechanical analysis method. Further, although the gabion structures were frequently used for stream regulation and slope stabilization in Taiwan, up to date there seemed not appropriate design criterion and analysis. Therefore, to capture a more real deformation response, this study presented a series of finite element analyses to investigate the deformation of loaded gabion structures. Finally,

[1] Associate professor, Department of Soil and Water conservation, National Chung-Hsing University, 40227, Taichung, Taiwan, R.O.C.(*Corresponding Author; Tel.: +886-4-2284-0381 ext 506; Fax: +886-4-2287-6851; Email: dglin@dragon.nchu.edu.tw)

[2] Doctoral Student, Department of Soil and Water Conservation, National Chung-Hsing University, Taichung, 40227, Taiwan, R.O.C.

[3] Professor, Department of Soil and Water conservation, National Chung-Hsing University, Taichung, 40227, Taiwan, R.O.C.

two evaluation equations for estimating the displacement of the front face of a loaded gabion structure were provided and enable a quick evaluation on the design of gabion structure in engineering practice.

APPLICATIONS OF GABION STRUCTURES

It was common to use gabion structure for the erosion protection of channel bed. Peyras et al. (1992) carried out one-fifth-scale model tests of stepped gabion spillways subjected to different types of water loads. The tests indicated for expected floods in excess of 1.5 m^3/sec/m the mesh and lacing must be strengthened whereas stepped gabion spillways can withstand flows up to 3 m^3/sec/m without great damage if setting of gabions complies with the code of practice. The tests also revealed some deformation of the gabions due to movements of the stone filling. Some advices were given by Les Ouvrages en gabions (1992) on preventing gabion deformation. It was indicated the stone quality and packing in the top layers and stone size (1.5 times larger than the mesh size) are crucial to the deformation of gabion

In the design of erosion protection, gabion mattress was frequently used to resist the erosion of channel bed. Due to the similarity of shape, roughness, unit weight and connection method for each single gabion unit, the engineers are able to formulate a simple equation to describe the hydraulic characteristics of gabion structure. Stephen (1995) proposed a design procedure to determine the required average diameter of infilling stone and the thickness of gabion mattress to maintain the stability of the structure based on the engineering manual of U.S. Army Corps of Engineers (1991a) and guide specifications of U.S. Army Corps of Engineers (1991b). It was found that the stability of gabion mattress is much more dependent on the size of filling stone than on the thickness of mattress.

Agostini et al., 1987 and Gray and Sotir, 1996 indicated the advantage of using gabion structure in engineering practice. The main merit of gabion structures are their excellent function of free drainage and which alternately prevents the accumulation of excess pore water pressure and the associated instability problem. Moreover, the high porosity of gabion structure allows the flow infiltration and silt deposition in the pore space and this is advantageous to the invasion and growth of local plants and the conservation of ecosystem. The gabion structure is characterized by its monolithic and continuous construction process, reinforced structure, flexibility, permeability, durability, noise proofing, and beneficial environmental impact. Gabion structure is considered as an ecological structure, for it merges into the natural environment. The stone filling and the layer of vegetation growing on surface of the structure increase its landscape and durability. The wire mesh is zinc galvanized and polyvinylchloride coated to resist the corrosion.

At present in Taiwan the construction of gabion structures were mainly implemented for the revetment and retaining wall. Nevertheless, due to the particular hydrology condition and geography environment the gabion structures can be failed by the misuses in stream regulation and gully erosion control. Figures 1 and 2 illustrate the major applications of gabion structures.

(a)

(b)

Nan-Tou County (a) Zhu-Shan Township, Xiu Lin, Da-Hu-Di gabion retaining structure (b) Zhong-Liao, Qing-Shui village roadside slope protection

Fig. 1 Gabion structures for retaining wall and slope protection in Taiwan

(a)Tao-Yuan County, Long-Tan, Nan-Keng creek

(b) Tai-Chung County, Tai-Ping City, Tou-Bian-Keng creek (with energy dissipation facility)

Fig. 2 Gabion structure for stream regulation work in Taiwan

MATERIAL PROPERTIES OF GABION STRUCTURES

Wire mesh of gabion

In general, the wire used is soft steel and zinc galvanized to international standard. Zinc galvanized provides long term protection for steel wire against oxidation. The zinc galvanized wire is coated with special *PVC* (Polyvinylchloride) of 0.4~0.6 mm thick to give full protection against the corrosion from heavily polluted environment. The wire is woven into double twisted hexagonal wire mesh. At the construction site, the wire mesh of a single gabion unit with dimension of $W \times H \times L$ (width×height×length) are opened and assembled as shown in Fig. 3(a) and (b). The single gabion unit can be subdivided into cells (with volume of 1 m^3 in general) by inserting diaphragms spaced 1 m from each other to strengthen the stiffness of structure and to facilitate its assembly. The opening of wire mesh and the lacing between frame and wire are illustrated in Fig. 3(c). Various dimensions of steel wire, wire mesh and gabion unit commonly used for gabion structure are summarized in Table 1.

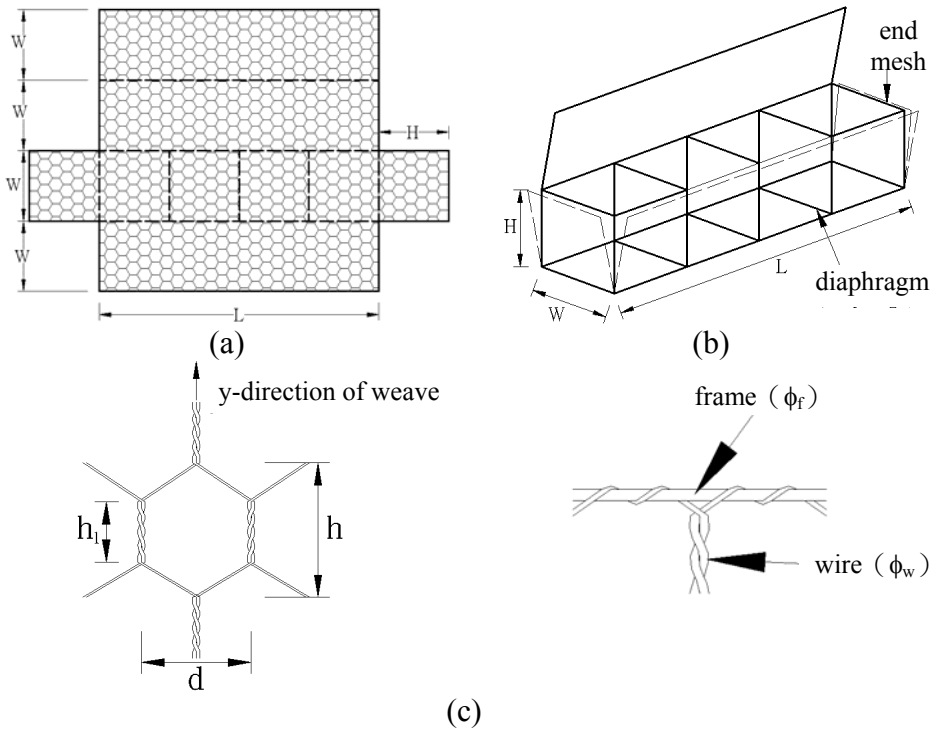

Fig. 3 Components of gabion unit (a) expansion of wire mesh (b) assembly of wire mesh (c) dimension of opening and lacing of frame and wire

Table 1 Dimensions of galvanized (zinc coated) wire and gabion unit (after foreign and Taiwan manufacturers)

Dimensions	Symbol	Unit	Specification
length	L	m	2.0/3.0/4.0/5.0
width	W	m	0.5/1.0/1.5/2.0
height	H	m	0.5/0.6/1.0/1.5
opening	$d \times h$	cm	5×8/8×10/10×15/15×20
twisted length	h_1	cm	4.5/6.0
diameter of wire	ϕ_w	mm	1.8/2.7/3.0/3.5
diameter of frame	ϕ_f	mm	3.0/3.5
thickness of *PVC* coating		mm	0.4～0.6

Infilling stone

Stone materials of higher unit weight γ_s are preferable particularly if the gravity function of the structure is predominant or if the structure is submerged or exposed to stream flow for a long period of time. To ensure the durability of the gabion structure the stone must has high resistance to weathering and erosion, and high compression strength. In addition, the apparent total unit weight γ_g ($=\gamma_s \times (1-n)$) required for various analyses can be determined by the unit weight of stone material γ_s and the porosity of the gabion n, which generally varies from 0.30 to 0.40 depending on the hardness and angularity of the stone. The most appropriate size for infilling stone d_s varies from 1and 1.5 to 2 times the dimension of the wire mesh d as shown in Fig. 3(c), namely, $d_s=(1\sim2)\times d$ and the stone should be large enough to avoid its escape through the opening of wire mesh. In general, the use of smaller sized stone, $d_s=(1\sim1.5)\times d$, permits an improved and more economical filling of the cage, it also allows a better distribution of the imposed loads and adaptability of the gabion structure to deformation.

NUMERICAL SIMULATIONS OF GABION STRUCTURES

The testing results of the uniaxial compression tests performed by Agostini et al. (1987) in the Structure Science Laboratory of the University of Bologna were used for numerical simulation.

Uniaxial compression tests of single gabion unit

1. Uniaxial compression tests

The single gabion unit used for uniaxial compression tests had nominal size of 0.5 m×0.5 m×0.5 m (=W×H×L or width×height×length) and were fabricated from 6 cm×8 cm (=d×h) woven hexagonal mesh of wire diameter 2.7 mm (=ϕ_w). The assembled gabion was filled by hand with quarried stone and compressed under lateral expansion unrestricted and restricted conditions as shown in Fig. 4. The figure displays the finite element model and deformation mode under two test conditions. The loading on the specimen was applied at a rate of 9.807 kN/m^2/min. and ceased when the mesh tended to be disintegrated. During the tests, the compression stress σ (=P/A) and compression strain ε (=$\Delta H/H_i$ and ΔH=H_i-H_f) were monitored. In which, P=compression loading, A=initial cross sectional area of gabion unit, H_i and H_f represent the initial and final height of gabion unit and ΔH=the finial compression displacement of gabion unit.

2. Numerical Simulation

The model parameters required for various material models were presented in Table 2. In numerical simulation, the wire mesh was modeled by a 5-nodes quadrilateral beam element and the corresponding axial stiffness E_s×A_s=1200 kN/m was employed. In which, the Young′s modulus of steel wire E_s=2×10^8 kPa and the cross sectional area of steel wire A_s= 6 mm^2 were used for a two dimensional plane strain model. Further, a relatively small flexural stiffness of steel wire E_s×I_s =12 kN×m^2/m (or merely ignore the flexural stiffness E_s×I_s=0 kN×m^2/m) was specified in the simulation to consider the deformation response of gabion structure with high flexibility.

In addition, a 15-nodes triangular soil element was used to model the infilling stone of gabion structure. The unit weight of infilling stone γ_s =25.5 kN/m^3 and the porosity n=0.3 were adopted to calculate the apparent total unit weight γ_g =(1–n)× γ_s =17.9 kN/m^3 of gabion structure. In numerical simulation, the unsaturated unit weight of filling stone γ_{unsat} = γ_g =17.9 kN/m^3 and the saturated unit weight of infilling stone γ_{sat}=19.6 kN/m^3 were assumed. Meanwhile, the effective cohesion c, effective friction angle ϕ and Poisson′s ratio ν of infilling stone were determined according to the range of strength parameters of stone material commonly used in engineering practice. The reduction coefficient R_{int}=0.7 was selected to compute the strength parameters c_{int} and ϕ_{int} (c_{int}=R_{int}×c and ϕ_{int}=R_{int}×tan^{-1}(tanϕ)) at the interface between wire mesh and filling stone. In such way, the relative displacement between wire mesh and infilling stone can be captured in numerical processes.

Table 2 Input model parameters of various material models used for gabion structure

Wire mesh panels						
Material Model	$E_s \times A_s$ (kN/m)			$E_s \times I_s$ (kN×m^2/m)		
Linear Elastic	1200			12		
Gabion with infilling stone						
Material Model	c (kN/m^2)	ϕ (°)	ν	γ_{unsat} (kN/m^3)	γ_{sat} (kN/m^3)	R_{int}
Mohr-Coulomb	20	35	0.3	17.9	19.6	0.7

In the numerical simulation of uniaxial compression test on single gabion unit, an apparent total tangential modulus E_t (=Δσ/Δε) from the experimental stress~strain curve (or σ~ε curve) was employed to represent the compound deformation characteristics of wire mesh and infilling stone instead of using the Young′s modulus of infilling stone itself (comparatively high). As listed in Table 3, the E_t of gabion structure was constantly adjusted in the numerical processes according to the compression stress level σ on the single gabion unit.

Table 3 Apparent total tangential modulus from experimental stress/strain curve of uniaxial compression test on single gabion unit at various compression stress levels (Agostini R. et al., 1987)

Stress dependent total apparent tangential modulus (restricted lateral expansion)				
σ (kN/m^2)	400	1020	1950	3380
E_t (kN/m^2)	2000	2800	4000	6000
Stress dependent total apparent tangential modulus (unrestricted lateral expansion)				
σ (kN/m^2)	200	450	900	1650
E_t (kN/m^2)	800	1200	2000	3000

As shown in Fig. 5, the simulations of stress~strain curve of uniaxial compression tests with unrestricted and restricted lateral expansion were compared with those from measurements given by Agostini R. et al. (1987). It can be seen the simulations are in good coincidence with the measurements although a slight deviation occurs in the case of unrestricted lateral expansion. The E_t modulus varied in the range of 1960~3920 kN/m^2 provided the compression strain ε remains smaller than about 30%. However, when ε greater than 30%, the curve rises sharply due to the core of the stone filling is progressively fractured and the external wire mesh increasingly mobilizes its containing function. A higher stiffness especially for small loads can be observed from the test and the simulation on specimen with restricted lateral deformation.

The behavior of the material may only be considered to be elastic when the levels of applied stress are low and it appears obvious when the gabions are loaded with restricted lateral deformation (or expansion). It should be noted that the gabions loaded in such a way as to prevent deformation on two opposite side mesh panels occurs frequently in practice, so that in some respects the compression tests on gabion units with restricted lateral deformation appear to be more significant than those of simple compression unrestricted lateral deformation. In a gabion structure the single gabion unit is confined by adjacent gabions which increase immeasurably retaining action to the mesh and this additional confinement action can double the uniaxial compression strength.

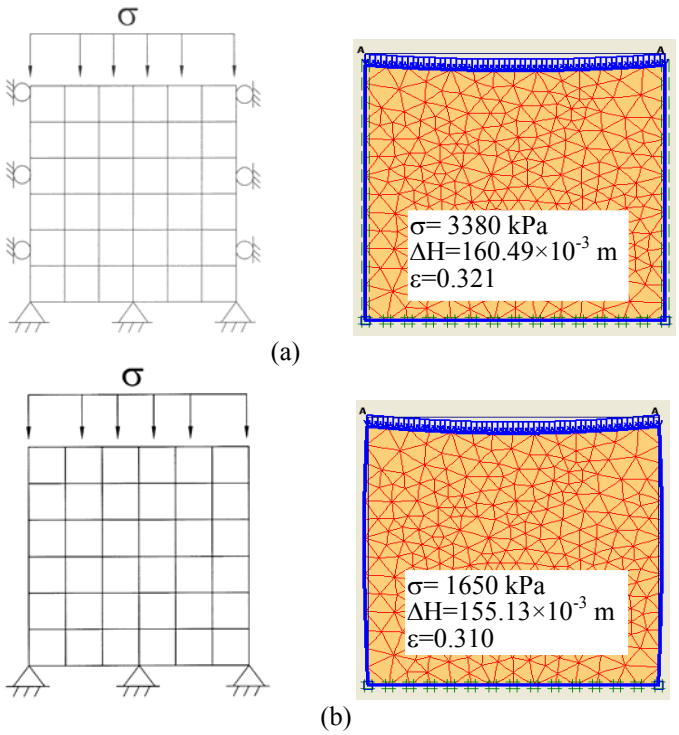

Fig. 4 Finite element numerical model and deformed mesh of uniaxial compression test on single gabion unit with (a) restricted (b) unrestricted lateral expansion

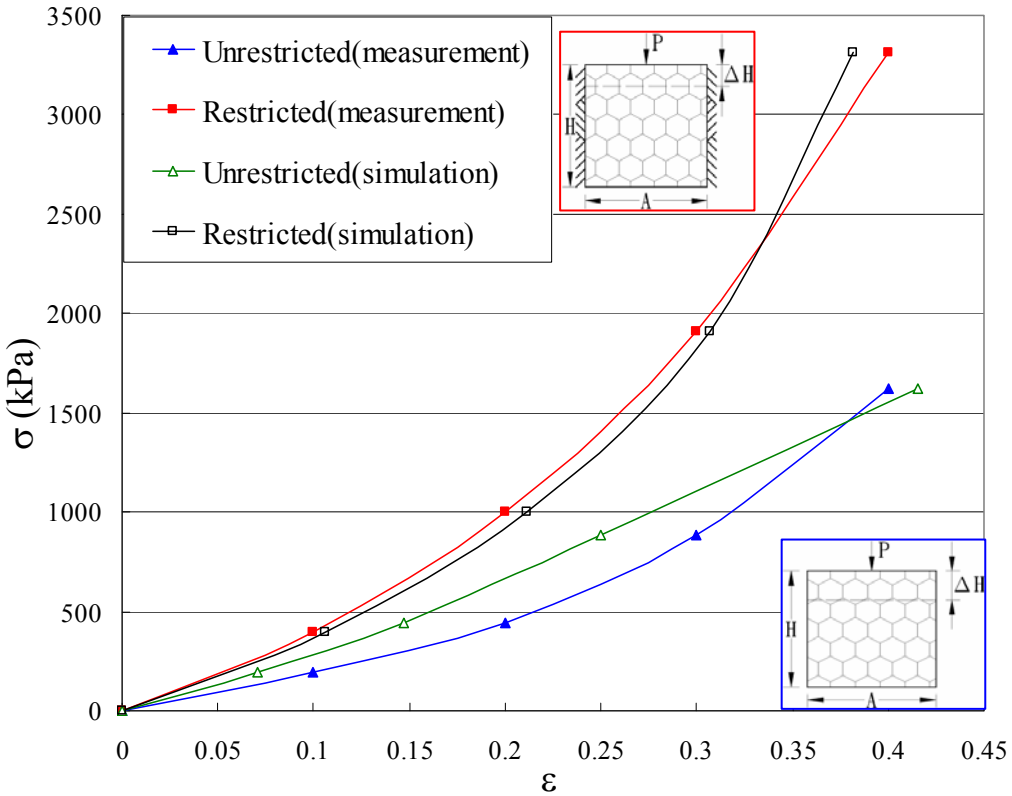

Fig. 5 The stress~strain curves of restricted and unrestricted lateral expansion uniaxial compression test on single gabion unit

Lateral loading test of full-scale gabion structure

The lateral loading test on a full scale 4 m high gabion wall was carried out at the Zola

Predosa factory of Officine Maccaferi S.p.A., near Bologna, Italy in collaboration with the Istituto di Tecnica delle Costruzioni of the University of Bologna. The detail of testing program and instrumentations were given by the Agostini R. et al. (1987).

1. Lateral Loading Test

Figure 6(a) illustrates the testing arrangement consisting of two gabion walls constructed oppositely each other and 1 m apart at the base. Wall structures were assembled by 1.5 m×1.0 m×1.0 m, 2.0 m×1.0 m×1.0 m and 1.5 m×1.0 m×0.5 m (=W×H×L or width×height×length) gabion units. The height of the wall was 4 m with bottom width of 2 m, a vertical front face, and a stepped back face that reduced the wall thickness to 1.5 m from the mid height to the top of the wall. The 0.5 m thick base platform extended 0.5 m on both sides and the total length of each wall was 5 m. The diameter of steel wire used for weaving wire mesh was 2.0 mm (=ϕ_w). The filling stone had an average diameter in the range of 90~120 mm (=d_s) and a friction angle ϕ=32° was assumed. The apparent total unit weight of gabion structure was estimated to be 17.7 kN/m^3 (=γ_g).

The ends of the space contained between the internal faces of the walls were closed off with steel plated interconnected by wire rope ties. Inside the enclosure was placed flexible water tanks arranged to form two separate chambers. Between the tanks and the interior faces of the walls was placed a 5 cm thick sheet of polystyrene to separate the tanks from the wire mesh and the ties which might have torn the tanks or interfered with their movement. The lateral loading was applied by pumping water into the tanks between the walls in successive increments. The loading test started on 1981/12/04 and a pressure head of 2.0 m was maintained in the duration from 1981/12/05 to 1981/12/15. Subsequently, the pressure head increased up to 3.4 m at 1981/12/16 and finally the pressure head reached a maximum of 4 m.

Figures 6(b) and (c) illustrates the acting forces on gabion walls and the conventional analysis method for lateral deformation calculation. In which, for an arbitrary elevation x_i from wall base, the shear force t_i was calculated according to the distribution of lateral pressure and the monitoring shear displacements Z_i and Z_{i-1} in respect to the elevations X_i and X_{i-1}. As a result, the shear strain γ_i can be computed by γ_i =[(Z_i-Z_{i-1})/(X_i-X_{i-1})]. The shear stress τ_i at elevations X_i was given by τ_i=(t_i/b_i) where b_i (or b) represents the thickness of gabion structure at elevation X_i. Eventually, the shear modulus G_i can be determined by G_i = (τ_i /γ_i).

As the aforementioned calculation procedures, through the monitoring lateral displacement Z_i one can determined the relation of the shear stress τ_i and the apparent total shear modulus of gabion wall G_i in term of G_i(τ_i)~τ_i (or G(τ)~τ) function as shown in Fig. 7. The linear equation presented in Fig. 7 has taken the structural flexibility of gabion into account in the formulation processes and the G_i modulus is relatively small compared with that of infilling stone itself. For an accurate analysis, the shear modulus of gabion wall G_i(τ_i) should be selected according to the shear stress level τ_i and the shear displacement Z_i is eventually calculated by [(τ_i /G_i)×b_i] or (γ_i×b_i). In practice, the shear stress τ_i carried by gabion structure is not significantly high and the stress/strain curve can be assumed linear. In such circumstances, a constant shear modulus G_i can be used to calculate the lateral displacement Z_i and for convenience the G_i modulus in the range of 245~343 kPa is considered to be rational for engineering practice.

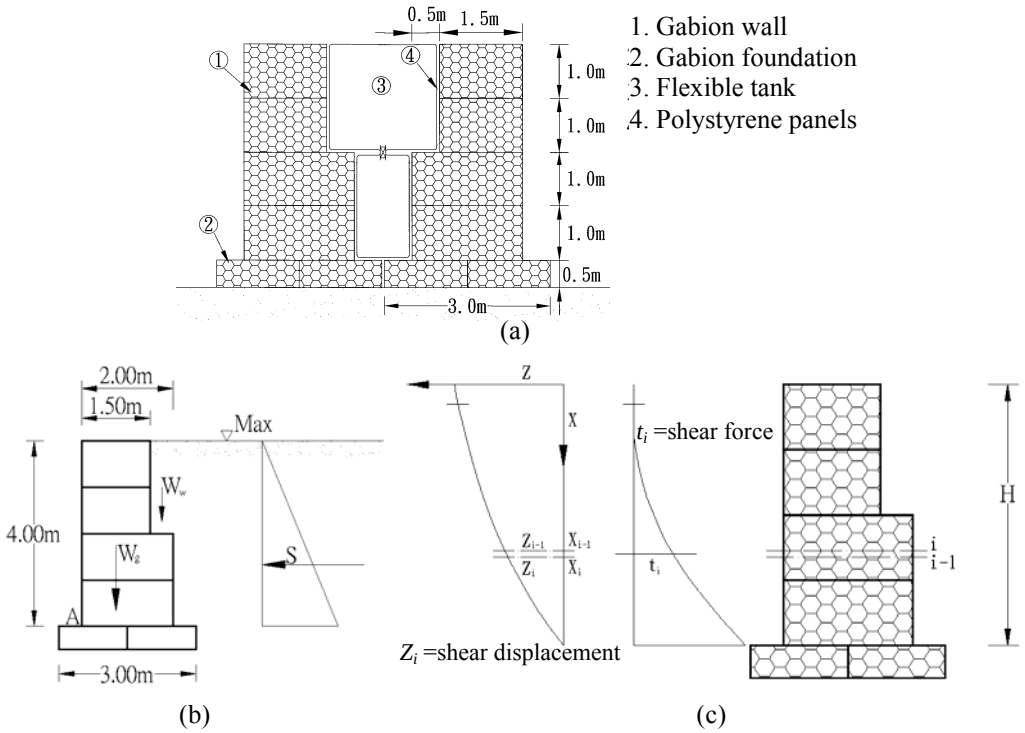

Fig. 6 Full scale lateral loading test on gabion structure (a) configuration of various components (b) force components (c) shear force and shear displacement

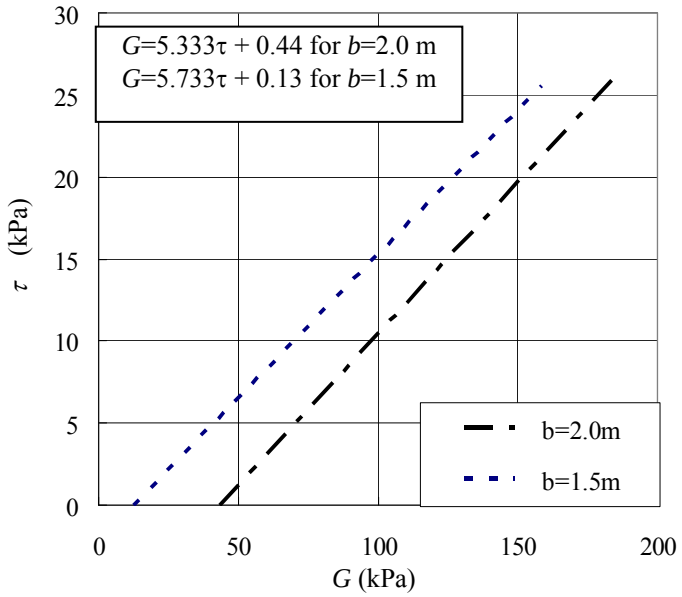

Fig. 7 Shear stress ~ apparent total shear modulus curve determined by lateral loading test on full scale gabion wall (after Agostini R. et al., 1987)

2. Numerical simulation

The gabion wall can be categorized as a gravity type structure with high flexibility and the interaction of shear displacement and ground settlement is the main deformation mode when subjected to lateral loading. However, the conventional analysis method is unable to handle the interaction behavior of gabion structure and foundation soil. This study attempted to capture the mechanic responses of loaded gabion structures in a more realistic way by numerical analysis technique. Meanwhile, to verify the effectiveness of numerical procedures, the numerical result of lateral displacement was compared with those from the measurements

given by Agostini R. et al. (1987). The finite element model for numerical analyses was established according to the configuration of lateral loading test in Fig. 6.

(1) Material model and model parameters

The stone filling and foundation soil were simulated by soil element with Mohr-Coulomb perfectly elastic-plastic model whereas the wire mesh was modeled by beam element with linear elastic model. To minimize the effect of ground settlement on the lateral deformation of gabion wall, a higher Young′s modulus for foundation soil was assumed in numerical simulation. The required parameters for Mohr-Coulomb model were summarized in Table 6. In the simulation, an apparent total shear modulus G=565 kPa (for restricted lateral expansion condition) was used and the corresponding apparent total Young′s modulus E equal to $[2\times(1+\nu)]\times G$=1470 kPa. In which, ν denotes the Poisson′s ratio of gabion wall. Moreover, the axial stiffness $E_s\times A_s$=660 kN/m and flexural stiffness $E_s\times I_s$=0 kN×m^2/m were inputted as the material parameters of wire mesh.

Table 6 Input model parameters of Mohr-Coulomb material model

Material Model Parameters	γ_{unsat} (kN/m^3)	γ_{sat} (kN/m^3)	c (kPa)	ϕ (deg.)	ν	E (kPa)	R_{int}
Gabion with stone filling	17.7	19.6	19.6	32	0.30	1470	0.7
Foundation soil	17.0	19.0	9.81	30	0.30	8160	0.7

(2) Implementation of numerical analyses

Totally, seven simulation phases were implemented to simulate the construction of gabion wall. *Phase-1*: in-situ stress calculation; *Phase-2*: construction of base gabion (0.5 m height); *Phase-3*~*Phase-6*: constructions of gabion wall (4 m of total height, 1 m height for each simulation phase); *Phase-7*: application of lateral loading.

(3) Numerical results

Figure 8 displays the deformation mode and the displacement fields of gabion wall subjected to lateral loading at final simulation phase.

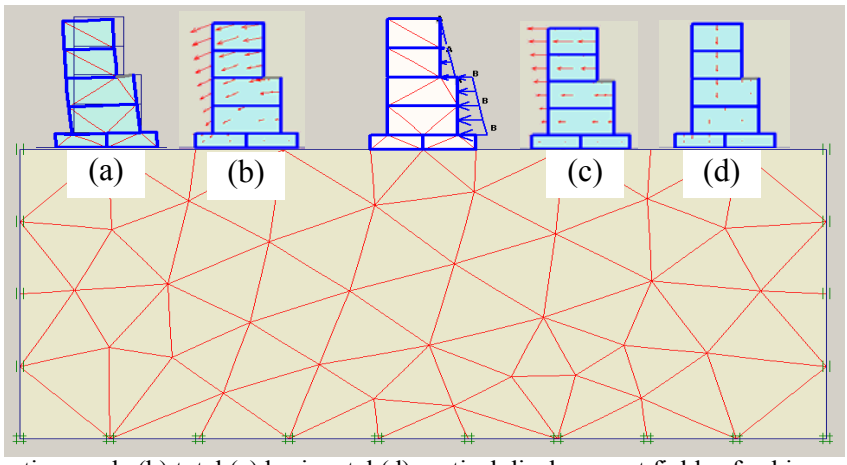

Fig. 8 (a) deformation mode (b) total (c) horizontal (d) vertical displacement fields of gabion wall subjected to lateral loading

Figure 9 presents the lateral displacements of wall surface from numerical simulations $\delta_{numerical}$, conventional analysis $\delta_{analytical}$ and measurement $\delta_{measurement}$ and the numerical result of settlement $S_{numerical}$. It was shown that the numerical procedures can successfully simulate

the lateral displacement of the loaded gabion wall. This repeatedly indicates that the apparent total shear modulus G (or the apparent total Young's modulus E) of gabion structure from various types of loading tests should be used in simulations rather than the shear modulus of filling stone itself (comparatively high).

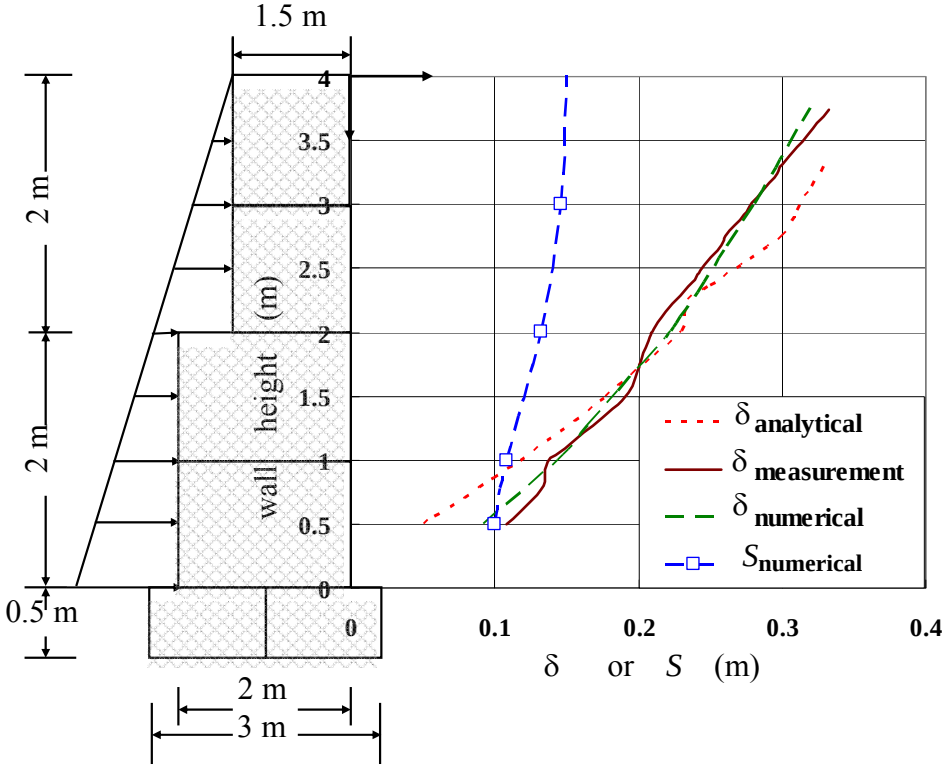

Fig. 9 Comparisons between calculations and measurements of lateral displacement of gabion wall from lateral loading test

PARAMETRIC STUDIES

The proposed numerical procedures for the displacement prediction of loaded gabion structures has been verified by the simulations of uniaxial compression tests on single gabion units and full-scale lateral loading test on a gabion retaining wall. Eventually, the back-calculated material model parameters in Table 6 were adopted for a series of numerical experiments on the gabion retaining structures with various configurations. As illustrated in Fig. 10, the stepped front face gabion retaining structure with height/width ratio $H/B \leq 1.5$ was selected for numerical investigation. The numerical variables include: wall height H=4, 6, 8, and 10 m; width of foundation base B=3, 4, 5, and 6 m; width of wall top b=1.5 m; and back-inclination angle of wall face α=6°. The simulation phase of wall construction was given as follows: *Phase-1*: initial stress calculation for a slope with inclination ratio of 1:1; *Phase-2*~*Phase-n*: constructions of gabion structure (construction height H=(n-1) m and backfill of the space between wall back and the slope surface.

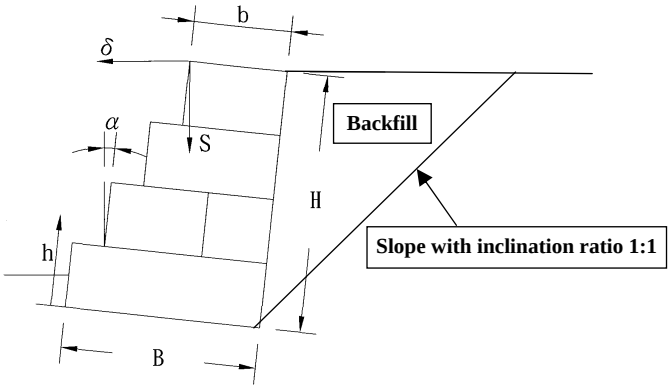

Fig. 10 Configuration variables of gabion structure

Deformation mode and maximum lateral displacement

As shown in Fig. 11, certain amount of vertical settlement (S) accompanies the horizontal displacement (δ) during the construction of gabion structure. The deformation mode exactly reflects the high flexibility of wire mesh and the structural adjustability. In addition, Fig 12 presents that the maximum vertical displacement ratio $(S_{max}/H)\times10^{-2}$ approximates 2.0~1.3 times of the maximum horizontal displacement ratio $(\delta_{max}/H)\times10^{-2}$ corresponding to a height/width ratio H/B=1.33~1.66 (S_{max} and δ_{max} in meters). This implies the designer should not ignore the accompanied vertical settlement when calculating the horizontal displacement of gabion structure by convention analysis method.

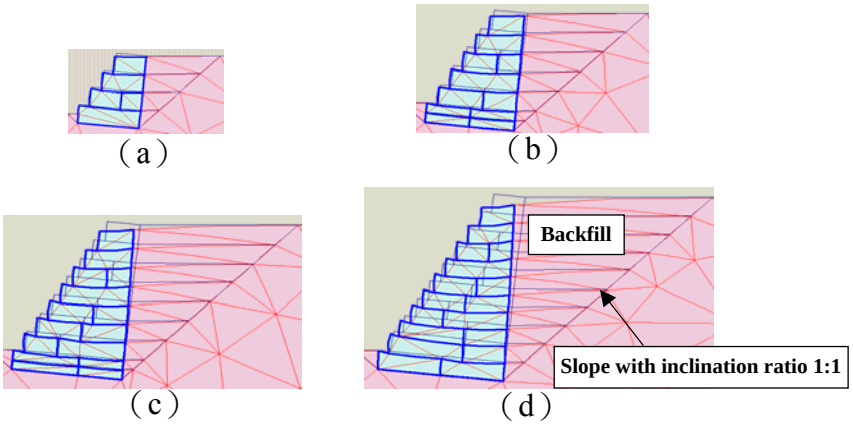

Fig. 11 Deformation mode of gabion structure with different configuration of (a)H= 4 m，B=3 m (b) H= 6 m，B=4 m (c) H= 8 m，B=5 m (d) H= 10 m，B=6 m

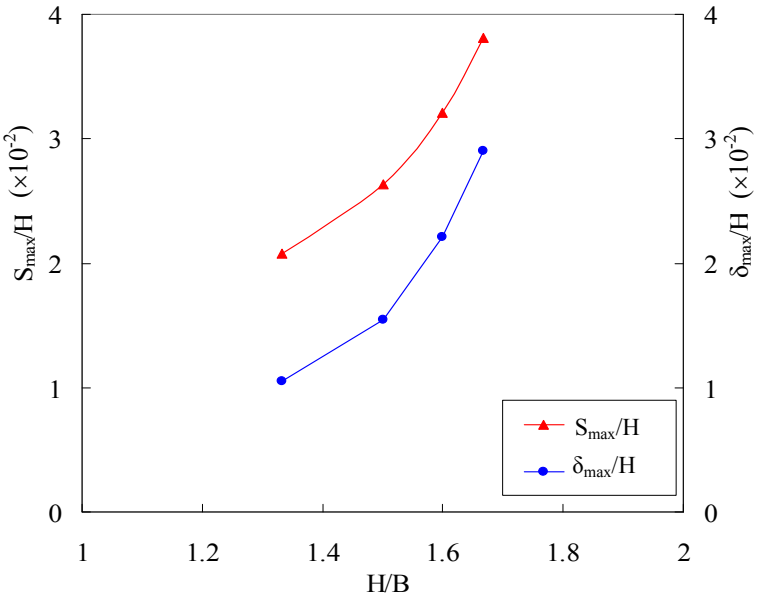

Fig. 12 Relationship of maximum horizontal (δ_{max}/H)×10^{-2} and maximum vertical (S_{max}/H) ×10^{-2} displacement ratio with height/width ratio (H/B) of gabion structure

Evaluation equations of displacement

As shown in Fig. 13, using the numerical results of horizontal and vertical displacement ratios (δ/H) and (S/H) (δ and S in meters) of the front face of gabion structure for regression analyses, two regression displacement equations expressed in term of elevation ratio (h/H) can be determined as follows:

$$\left(\frac{\delta}{H}\right) = \left(0.002 \times H^{1.2}\right) \times \left(\frac{h}{H}\right) \quad \text{(m)}$$

$$\left(\frac{S}{H}\right) = \left(0.008 \times H^{0.75}\right) \times \left(\frac{h}{H}\right) \quad \text{(m)}$$

For a similar field condition and construction case, the above equations enable a prediction of the displacement distribution of a loaded gabion structure at preliminary design stage.

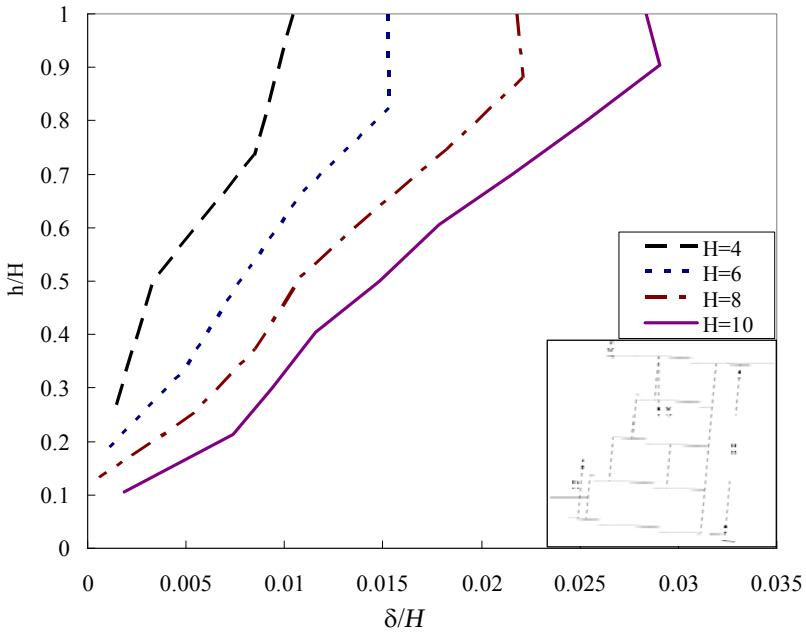

(a)

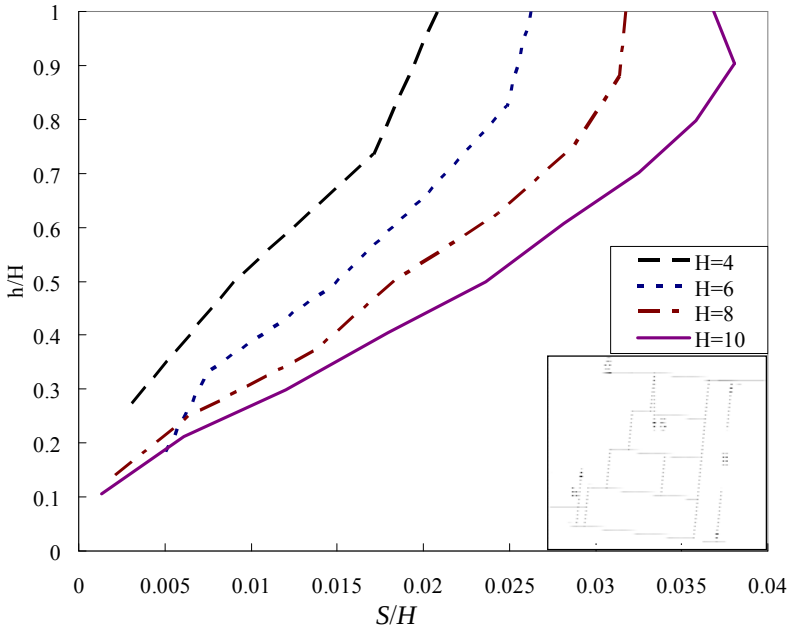

(b)

Fig. 13 Displacement distributions at the different elevation of the front face of gabion structure (a) horizontal ratio (δ/H) (b) vertical displacement ratio (S/H)

CONCLUSIONS

Based on the numerical analyses, several conclusions can be drawn:

1. In numerical modeling, a beam element with limit axial stiffness and relatively low flexural stiffness enables an excellent simulation of the behavior of wire mesh with high flexibility. Further an apparent total shear modulus G (or Young′s modulus E) of gabion structure which can capture the compound deformation behavior of wire mesh and filling stone should be used for analyses instead of the shear modulus of filling material itself (extremely high).
2. The maximum vertical displacement ratio $(S_{max}/H)\times10^{-2}$ approximates 2.0~1.3 times of the

maximum horizontal displacement ratio (δ_{max}/H)×10^{-2} for a gabion retaining structure with wall height/base width ratio H/B=1.33~1.66 when subjected to construction loading. This inferred that the vertical displacement should not be disregarded when designers calculated the horizontal displacement by the conventional analysis method.

3. The presented displacement equations, namely, the (δ/H)~(h/H) and (S/H)~(h/H) relationships were applicable to those construction cases with similar field conditions for the evaluations of displacement at preliminary design stage.

REFERENCES

Agostini R., Cesario L., Conte A., Masetti M., and Papetti A. (1987). "Flexible gabion structures in earth retaining works," *Officine Maccaferri S.p.A.*, Bologna, Italy.

Gray H. and Sotir B. (1996). "Biotechnical and Soil Bioengineering Slope Stabilization, A Practical Guide for Erosion Control," *A Wiley-Interscience Publication*, John Wiley and Sons, Inc.

Les Ouvrages en gabions (1992). "Collection techniques rurales en Afrique," *Minist'ere de la Coop'eration* , Paris, France (in French)

Officine Maccaferri S.p.A. (1997). "Terramesh System-A solution for soil-reinforcement," Bologna, Italy.

Peyras L., Royet P., and Degoutte G. (1992). "Flow and Energy Dissipation over Stepped Gabion Weirs," *Journal of Hydraulic Engineering*, *ASCE*, Vol. 118, No. 5, May, pp. 707~717.

Stephen T. Maynord (1995). "Gabion-Mattress Channel-Protection Design," *Journal of Hydraulic Engineering*, *ASCE*, Vol. 121, No. 7, July, pp. 519~522.

U.S. Army Corps of Engineers (1991a). "Hydraulic design of flood control channels, Engineer Manual 1110-2-1601," *U.S. Government Printing Office*, Washington, D.C.

U.S. Army Corps of Engineers (1991b). "Wire mesh gabion," *Civil Works Construction Guide Specification CW-02541*, 29 July 1991, U.S. Government Printing Office, Washington, D.C.